Available online at www.sciencedirect.com
SCIENCE DIRECT
Trans. Nonferrous Met. Soc. China 16(2006) 438−444
Transactions of Nonferrous Metals Society of China
www.csu.edu.cn/ysxb/

Phase transition of lithiated-spinel $Li_2Mn_2O_4$ at high temperature

TANG Xin-cun(唐新村)[1, 2], HUANG Bai-yun(黄伯云)[2], HE Yue-hui(贺跃辉)[2]

1. School of Chemistry and Chemical Engineering, Central South University, Changsha 410083, China
2. State Key Laboratory of Powder Metallurgy, Central South University, Changsha 410083, China

Received 9 June 2005; accepted 26 September 2005

Abstract: The phase transition of $Li_2Mn_2O_4$ spinel at high temperature was investigated by XRD, TG/DTA, average oxidation state of Mn and cyclic voltammeric techniques. The results reveal that the $Li_2Mn_2O_4$ spinel is unstable. At high temperature, it is easy to transform into $[Li_{2-2x}]_{tet}[Mn_{2-x}Li_x]_{oct}O_4$, which accompanies the formation of Li_2MnO_3 impurities. The phase transition is associated with the transfer of Li^+ from tetrahedral 8a sites to octahedral 16d sites. With the increasing sintering temperature from 450 ℃ to 850 ℃, the phase structure varies from lithiated-spinel $Li_2Mn_2O_4$ to $Li_4Mn_5O_{12}$-like to $LiMn_2O_4$-like and finally to rock-salt $LiMnO_2$-like. In addition, a way of determining x with average oxidation state of Mn and the content of Li_2MnO_3 was also demonstrated.

Key words: lithium manganese oxide; $Li_2Mn_2O_4$; phase transition; lithium-ion batteries

1 Introduction

Lithium manganese oxides are the most attractive cathode materials for rechargeable lithium-ion batteries because of their low-cost and less toxicity when compared with either cobaltates or nickelates[1−3]. Among these oxides, the spinel-framework compounds have been widely investigated due to scientific and commercial interest. In the ideal spinel $LiMn_2O_4$, Li and Mn respectively occupies tetrahedral 8a and octahedral 16d sites with space group Fd3m; and Li intercalates or deintercalates reversibly from 8a sites, which offers a theoretical capacity of 148 mAh/g with two charge/discharge plateaus at about 3.95 V and 4.15 V (vs Li^+/Li). However, the poor rechargeability restricts its commercial applications. A number of studies have been done to improve its rechargeability, for example, by replacing Mn with other alloying elements[4, 5]. In particular, spinels $Li_{tet}[Mn_{2-x}Li_x]_{oct}O_4$, by replacing Mn with Li, have given rise to widely interests[6−8].

It is known that Li not only can substitute partially Mn in the octahedral 16d sites to form the manganese-absent spinels $Li_{tet}[Mn_{2-x}Li_x]_{oct}O_4$ ($0 \leqslant x \leqslant 0.33$) but also can further occupy the unoccupied tetrahedral 8a sites to form the lithium-rich spinels $Li_{1+y}Mn_2O_4$ ($0 \leqslant y \leqslant 1$). As a result, a series of spinel $Li_{1+x+y}Mn_{2-x}O_4$ compounds are given in the Li-Mn-O phase diagram with the average valent of Mn varied from 3 to 4[1, 9, 10]. For examples, at x = 0 and y = 1, the stoichiometric compound is the lithiated-spinel $Li_2Mn_2O_4$ in which all Mn is trivalent, and it exhibits three voltage plateaus during the Li^+ intercalation/ deintercalation respectively in about 3.0, 3.95 and 4.15 V[6, 11]; and at x = 0.33 and y = 0, the stoichiometric compound is given as $Li_4Mn_5O_{12}$, in which all Mn is tetravalent; it offers a theoretical capacity of 163 mA·h/g in 3 V region and no capacity in the 4 V region[12−14]. From a structural point of view, when the oxidation state of Mn falls below 3.5, the Jahn-Teller distortion occurs and consequently deteriorates the rechargeability of spinel compounds. Thus, the spinels $Li_{1+x+y}Mn_{2-x}O_4$ with high values of x and low values of y (e.g. $Li_4Mn_5O_{12}$) have been adapted to increase the average valence of Mn and further to improve the rechargeability. However, as suggested previously by various authors[7,12,14], the spinels $Li_{1+x+y}Mn_{2-x}O_4$ with high values of x are less thermo-stable than those with lower values of x at higher sintering temperature. For this purpose, the phase transition of the lithiated-spinel $Li_2Mn_2O_4$ at high

Foundation item: Project(20406024) supported by the National Natural Science Foundation of China; Project(76600) supported by the Postdoctoral Science Foundation of Central South University, China
Corresponding author: TANG Xin-cun; Tel: +86-731-8836961; E-mail: tangxincun@163.com

temperatures was investigated in this work.

2 Experimental

2.1 Preparation of lithium manganese oxide

$LiMnC_2O_4$(Ac) precursor was prepared by the method of the low-heating solid-state reaction as similar to the literature[15, 16]. The lithium manganese oxides were prepared by sintering the $LiMnC_2O_4$(Ac) precursor in air at different temperatures for 12 h with the heating rate of 10 ℃/min, without intermediate regrinding or other heating treatments.

2.2 Measurements and characterizations

The thermogravimetry (TG) and differential thermogravimetry(DTG) curves were recorded on a PE-DTG/1700 thermal analyzer with a heating rate of 10 ℃/min. The X-ray powder diffraction patterns were recorded with a Rigaku D/Max-3B X-ray diffractometer, Cu K_α. The average oxidation state of Mn in the Li-Mn-O spinel products was determined by the redox titration with oxalic acid as reducing agent and the hot sulfuric acid as solvent of Li-Mn-O spinel, and the excess oxalate acid was back-titrated by potassium permanganate solution. The cyclic voltammetric(CV) curves of Li-Mn-O spinels were recorded on the CHI660 Electrochemical Workstation with the scan rate of 0.02 mV/s by using the powder microelectrode(PME) as working-electrodes. PMEs used in this work were made from Pt micro-disk electrodes of 0.1 mm in diameter. Pt micro-disk electrode was first chemically etched to form a cavity of tens of micrometers deep and then the cavity was filled with Li-Mn-O spinels powder without any binder and conductive. All cell handing was performed in an argon-filled glove box. Lithium was used as both the negative electrode and the reference electrode, 1 mol/L LiPF6 dissolved in a mixture of propylene carbonate(PC) and dimethoxyethane(DME) (PC ： ME=1 ： 1, by volume) was used as the electrolyte.

3 Results and discussion

Fig.1 shows the TG and DTA curves of the precursor $LiMn(C_2O_4)$(Ac). The TG curve indicates that the mass loss occurs mainly in two steps in the temperature range of 100-487℃. In the first step, the mass loss of 7.31% is associated with the departure of methyl (cal. 7.20%) in the temperature range of 100−190 ℃, and the small exothermic peak is correspondingly observed at around 190℃ in the DTA curve. In the second step, the mass loss of 48.82% in the temperature range of 190−487 ℃ corresponds to the combustion of residual organic constituents (47.87%, calculated according to the $Li_2Mn_2O_4$ product) in precursor, which accompanies a strong exothermic peak at 274 ℃ in the DTA curve. The total mass loss in the temperature range of 100−487 ℃ is measured as 56.13%, which is in good accordance with the calculated value of 55.07% within the experimental error. These results suggest that the organic elements (C and H) in $LiMn(C_2O_4)$(Ac) are completely decomposed in this temperature range. The detailed thermo-decomposed processes are shown in Fig.2. In addition, there is a little mass loss of about 2% between 487 ℃ and 900 ℃, which is resulted from the worse stability of Li-Mn-O spinels with high Li/Mn ratio at high temperature.

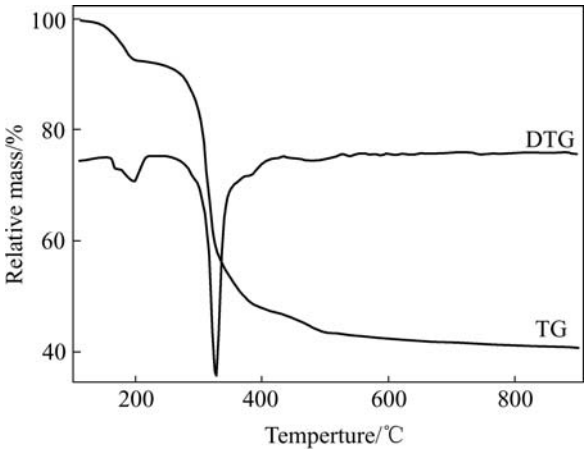

Fig.1 TG-DTG curves of $LiMn(C_2O_4)$ (Ac) precursor measured with heating rate of 10℃/min

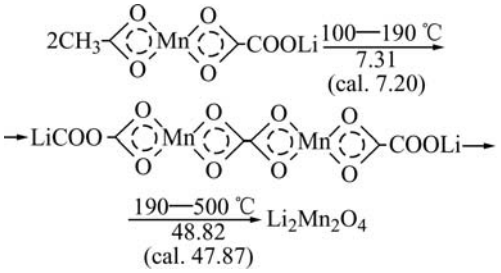

Fig.2 Thermo-decomposition process of $LiMn(C_2O_4)$(Ac)

Fig.3 shows the powder XRD patterns of the Li-Mn-O samples prepared by sintering the $LiMn(C_2O_4)$(Ac) precursor at 450, 500, 550, 600, 700 and 850 ℃. According to the typical XRD patterns of the various Li-Mn-O compounds summarized by JULIEN et al[17], except for the marked peaks indicating the corresponding impurities, the mainly diffraction peaks can be indexed by the cubic spinel unit cell (Fd3m). For the 450 ℃ sample, a small amount of the orthorhombic $LiMnO_2$ (Pmmn) and tetragonal $Li_2Mn_2O_4$ ($F4_1/ddm$) can be respectively observed from the diffraction peaks at 2θ=25.10° (marked by ▲) and at 2θ=32.76° (marked by ◦)[11,17]. When the sintering temperature increases to 500 ℃, the orthorhombic $LiMnO_2$ impure phase disappears, whereas the rock salt

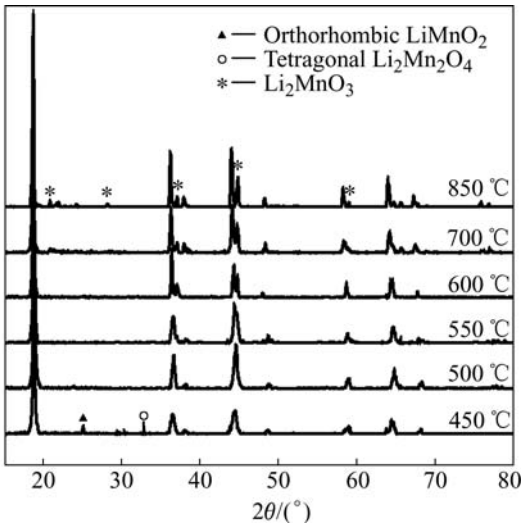

Fig.3 XRD patterns of Li-Mn-O spinel prepared by sintering precursor at various temperatures for 12 h in air

Li_2MnO_3 impurities (C2/m, especially at about 2θ =37.10° and 44.80°, marked by *) emerges when the sintering temperature is above 550 ℃[12,13,17]. Considering 1∶1 Li/Mn ratio in the $LiMn(C_2O_4)(Ac)$ precursor, it was judged that the 450 ℃ sample mainly consisted of the lithiated-spinel $Li_2Mn_2O_4$. However, for $[Li_{1+y}]_{tet}[Mn_{2-x}$- $Li_x]_{oct}O_4$ spinel series with high Li/Mn ratio, the similar oxygen array even if the different molar fraction and different occupied site fraction (8a or 16d) of lithium, made them difficult to be identified distinctly by the closely similar XRD patterns[17], especially at the disturbance of the phase of Li_2MnO_3 impurities. As reported by several authors[6,13,17, 20], the cell parameters and the electrochemical properties have more distinct differences among these $[Li_{1+y}]_{tet}[Mn_{2-x}Li_x]_{oct}O_4$ spinel series. For some stoichiometric Li-Mn-O compounds, these differences are summarized in Table 1.

Fig.4 shows the CV curves of the Li-Mn-O spinels obtained by sintering $LiMn(C_2O_4)(Ac)$ precursor at various temperatures. It is seen from the CV curves that the potentials of Li^+ intercalation/ deintercalation (vs Li^+/Li) have distinct difference among these Li-Mn-O samples. The data of the cell parameters (calculated from Fig.5 with reference to the cubic spinel unit cell) and potentials of Li^+ intercalation/ deintercalation for the Li-Mn-O samples obtained at different sintering temperatures are given in Table 2. It can be seen that the lattice parameter decreases firstly in the sintering temperature range from 450 ℃ to 550 ℃ and then increases in the sintering temperature range from 550 ℃ to 850 ℃. Because of the Jahn-Teller effect of Mn^{3+} in $Li_2Mn_2O_4$ for 450 ℃ sample, a slight distortion from cubic to tetragonal unit cell is also observed from the cell parameters (a=8.146 Å, c=8.480 Å, c/a=1.04) calculated from the Miller indices of the tetragonal unit cell. By comparing the data of cell parameters and potential of Li^+ intercalation/deintercalation in Table 1 with that in Table 2, the phase structure of the Li-Mn-O samples obtained at different sintering temperatures can be judged as given in Table 3.

From the XRD patterns in Fig.3, the intensities of diffraction peaks of Li_2MnO_3 increase clearly with the raising sintering temperature, which indicates that the content of Li_2MnO_3 in the Li-Mn-O spinels increases with the sintering temperature. Clearly, the formation of Li_2MnO_3 impurities must lead to the variation of the composition of the Li-Mn-O samples because the Li/Mn

Table 1 Data of cell parameters and potential of Li^+ intercalation/deintercalation for some stoichiometric Li-Mn-O compounds

Compound	Structure	Cell parameters/Å	Potential of Li^+ intercalation/deintercalation(vs Li^+/Li)/V
$LiMn_2O_4$[17, 20]	Cubic	a=8.245	3.9/4.0, 4.05/4.15, two redox couples
$Li_4Mn_5O_{12}$[13, 17]	Cubic	a=8.137	2.8/3.5, one redox couple
$Li_2Mn_2O_4$[6, 17]	Tetragonal	a=7.994, c=9.329	2.5/3.0, 3.9/4.0, 4.05/4.15, three redox couples
o-$LiMnO_2$[17,19]	Orthorhombic	a=2.806, b=5.750, c=4.593	2.5/3.0, one redox couple *
Li_2MnO_3[18]	Monoclinic	a=8.12**	3/3.5, one redox couple

*Transformation into spinel during cycle leads to potentials in 4V region; **: calculated from cubic settings

Table 2 Cell parameters, potential of Li^+ intercalation/ deintercalation and average oxidation state of Mn for Li-Mn-O samples obtained at different sintering temperatures

Sintering temperature/℃	Cell parameters/Å	Potential of Li^+ intercalation/deintercalation(vs Li^+/Li)/V	Average oxidation state of Mn
450	8.163(a=8.146, c=8.480)*	2.68/3.01, 3.30/3.72, 3.76/4.04	3.12
500	8.137	2.60/3.21	3.67
550	8.131	3.10/2.68, 3.82/3.68	3.71
600	8.187	3.78/3.36, 3.06/2.9, 2.42	3.64
700	8.203	3.86/3.66, 3.56/3.28, 2.97/2.65	3.59
850	8.216	3.21/2.53	3.52

* Calculated with reference to the tetrahedral unit cell

Table 3 Structure properties of Li-Mn-O samples obtained at different sintering temperatures

Sintering Temperature/℃	Structure of main products	Impurities
450	Cubic $Li_2Mn_2O_4$, with slightly tetragonal distortion	O-$LiMnO_2$ Tetragonal $Li_2Mn_2O_4$
500	Similar to $Li_4Mn_5O_{12}$	-
550	Similar to $Li_4Mn_5O_{12}$	Li_2MnO_3
600	Between $Li_4Mn_5O_{12}$ and $LiMn_2O_4$	Li_2MnO_3
700	Similar to $LiMn_2O_4$	Li_2MnO_3
850	Similar to rock-salt $LiMnO_2$	Li_2MnO_3, Mn_3O_4

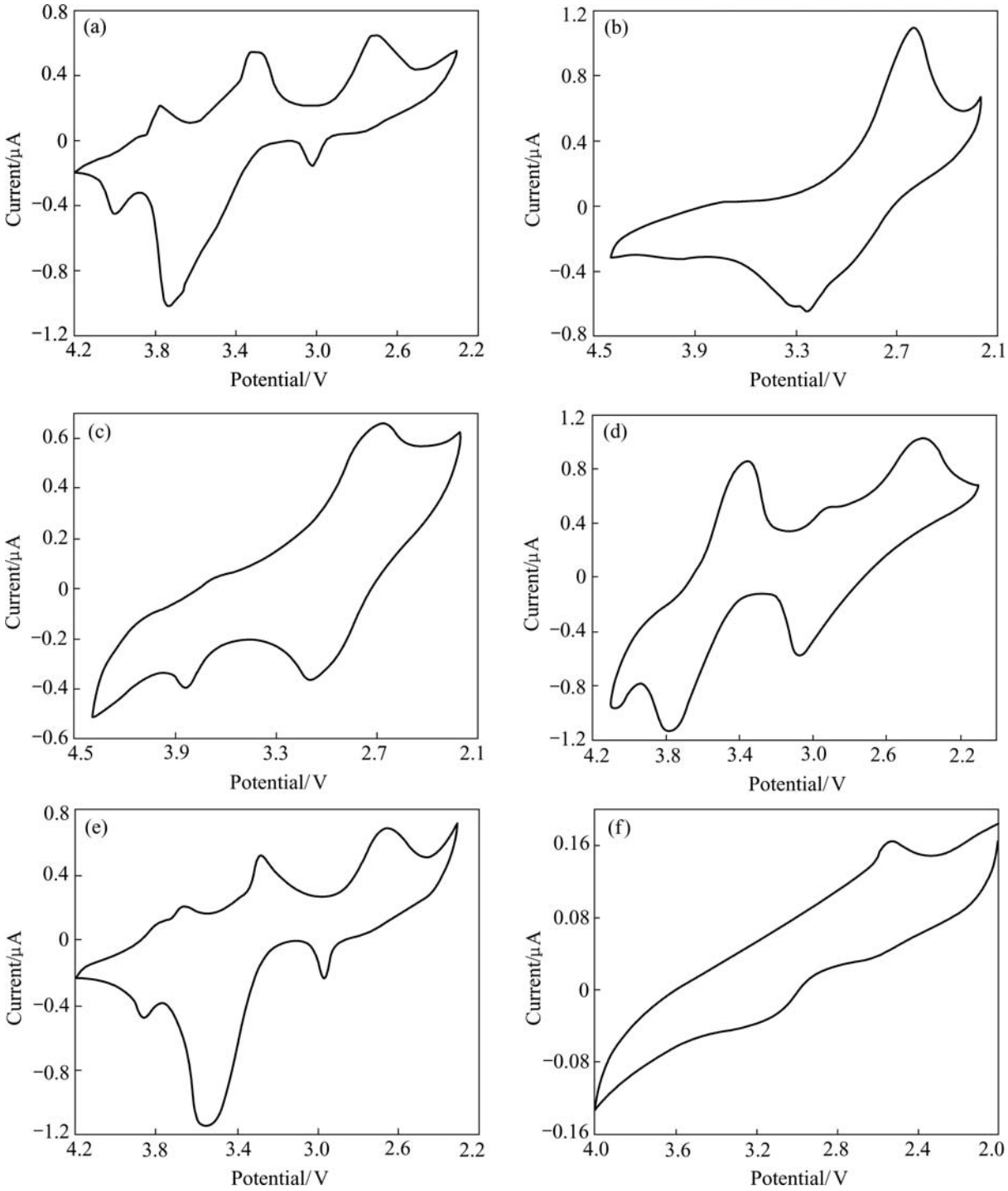

Fig.4 CV curves of Li-Mn-O spinels prepared by sintering precursor at different temperatures: (a) 450 ℃; (b) 500℃; (c) 550 ℃; (d) 600 ℃; (e) 700 ℃; (f) 850 ℃

ratio for Li_2MnO_3 is as twice times as the nominal Li/Mn ratio in the $LiMn(C_2O_4)(Ac)$ precursor, and consequently lead to the phase transition of the Li-Mn-O spinels. Fig.5 shows the TG curve of $Li_2Mn_2O_4$ (450 ℃ sample) in the heating temperature range from 300 ℃ to 850 ℃. It is observed that the mass increases gradually between 320 ℃ and 540 ℃ with about 2.41% increment. Because of the instability of the lithiated-spinel $Li_2Mn_2O_4$ at high temperature resulted from the Jahn-Teller distortion, it decomposes under the oxidizing conditions of an air atmosphere. However, the mass loss between 540 ℃ and 850 ℃ shown in Fig.5 indicates a more complicated phase transition process.

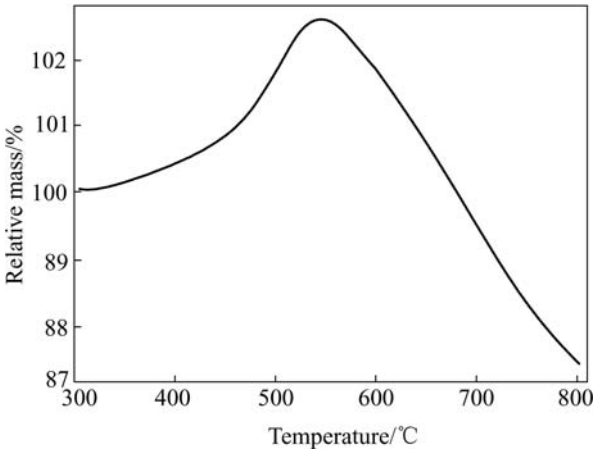

Fig.5 TG curve of 450 ℃ sample, measured with heating rate of 10 ℃/min

According to the formation of the Li_2MnO_3 impurities, the reaction equation can be expressed as

$$(3-3x-y)/2\ Li_2Mn_2O_4+(1-y)/2O_2\rightarrow [Li_{1+y}]_{tet}[Mn_{2-x}Li_x]_{oct}O_4+(1-2x-y)Li_2MnO_3 \quad (1)$$

where x is the fraction of Li^+ occupied in the octahedral 16d sites, and y is the fraction of Li^+ occupied in tetrahedral 8a sites. Here, $[Li_{1+y}]_{tet}[Mn_{2-x}Li_x]_{oct}O_4$ formula was based on the fact that Li not only can substitute partially Mn in the octahedral 16d sites to form the manganese-absent spinels but also can occupy the unoccupied tetrahedral 8a sites to form the lithium-rich spinels. From Eqn.(1), the uptake oxygen leads to the increase of mass, as is confirmed by the TG curve in Fig.5. According to Eqn.(1), it is considered having two cases as follows

1) For the case of $2x+y=1$

In this case, Li_2MnO_3 phase does not form. The oxidization of $Li_2Mn_2O_4$ is only resulted from the transfer of Li^+ from tetrahedral 8a sites to octahedral 16d sites. By substituting $y=1-2x$ into Eqn.(1), as a result, Eqn.(1) can be expressed as

$$(1-x/2)Li_2Mn_2O_4+xO_2\rightarrow [Li_{2-2x}]_{tet}[Mn_{2-x}Li_x]_{oct}O_4 \quad (2)$$

This reaction equation can also be expressed as an oxygen-rich form:

$$Li_2Mn_2O_4+\delta O_2\rightarrow Li_2Mn_2O_{4+\delta} \quad (3)$$

Clearly, the average oxidation state of Mn in $Li_2Mn_2O_{4+\delta}$ is higher than that in $Li_2Mn_2O_4$, but the Li/Mn ratio is not varied. With the increasing x value, $Li_2Mn_2O_4$ can be oxidized and gradually transited to a middle-phase similar to stoichiometric $Li_4Mn_5O_{12}$. As shown in Table 3, the 500 ℃ sample should be categorized to this case. Because the average oxidation state of Mn is increased, the thermal stability of $[Li_{2-2x}]_{tet}[Mn_{2-x}Li_x]_{oct}O_4$ is improved. According to Eqn.(2), the average oxidation state of Mn, n, can be expressed as

$$n=\frac{8}{2-x}-1 \qquad (0\leqslant x\leqslant 0.333) \quad (4)$$

or

$$\begin{cases} x=2-\dfrac{8}{n+1} \\ y=\dfrac{16}{n+1}-3 \end{cases} \qquad (3\leqslant n\leqslant 3.8) \quad (5)$$

Fig.6 shows the functions of $x-n$ and $y-n$ for this case. Therefore, the fraction of Li^+ in the octahedral 16d sites can be calculated from the average oxidation state of Mn. For the ideal cubic $Li_2Mn_2O_4$ (x=0, y=1) in which all of lithium-ions occupy in the tetrahedral 8a sites, n is 3. In the case of x=0.333, $[Li_{2-2x}]_{tet}[Mn_{2-x}Li_x]_{oct}O_4$ exhibits the ideal lithium-rich $Li_{4+y}Mn_5O_{12}$ phase (y=1). The maximal value of n could reach 3.8 if the ratio of Li/Mn in $[Li_{2-2x}]_{tet}[Mn_{2-x}Li_x]_{oct}O_4$ would retain at 1:1 until x=0.333. For examples of 450 ℃ sample and 500 ℃

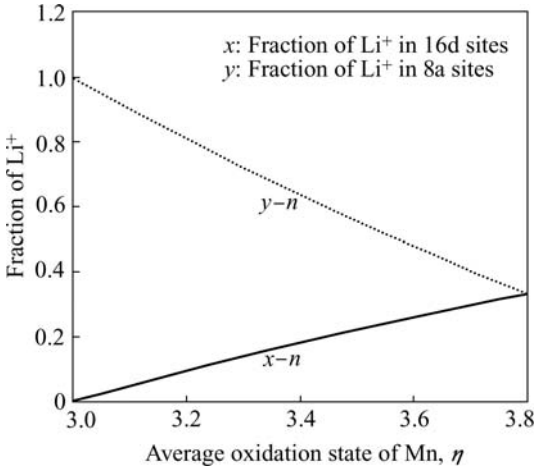

Fig.6 Function of average oxidation state of Mn with fraction of Li^+ in octahedral 16d sites ($x-n$) and tetrahedral 8a sites ($y-n$) for $[Li_{1+y}]_{tet}[Mn_{2-x}Li_x]_{oct}O_4$ spinels (Li:Mn=1, at case of $2x+y=1$)

sample, the XRD data in Fig.3 suggest the Li_2MnO_3 phase does not clearly form. From their average oxidation state of Mn as given in Table 2, it can be estimated that the x of Li^+ in the octahedral 16 d sites is ab. 0.06 for 450 ℃ sample and 0.287 for 500 ℃.

2) For the case of $2x+y\leqslant 1$

In this case, Li_2MnO_3 phase forms. The reaction as Eqn.(1) increases the average oxidation state of Mn and also lowers the Li/Mn ratio in the $[Li_{1+y}]_{tet}[Mn_{2-x}Li_x]_{oct}O_4$ spinel phase. As a result, the thermal stability of $[Li_{1+y}]_{tet}[Mn_{2-x}Li_x]_{oct}O_4$ spinel is further enhanced with the separation of the more stable Li_2MnO_3. According to the structure properties in Table 3, the 550 ℃ samples should be approximately categorized to this case. From Eqn.(1), the average oxidation state of Mn in the multiphase of $[Li_{1+y}]_{tet}[Mn_{2-x}Li_x]_{oct}O_4$ and Li_2MnO_3 can be expressed as

$$n=\frac{11-9x-5y}{3-3x-y} \quad ((0\leqslant x\leqslant 0.333) \tag{6}$$

Assuming the molar ratio of $Li_{1+y}]_{tet}[Mn_{2-x}Li_x]_{oct}O_4$ spinel to Li_2MnO_3 phase is m, from Eqn.(1), the value of m can be expressed as

$$m=1-2x-y \tag{7}$$

Substituting Eqn.(7) into Eqn.(6), the fractions of Li^+ in tetrahedral sites and in octahedral sites can be respectively calculated from

$$\begin{cases} x=\dfrac{mn+2n-5m-6}{n+1} \\ y=\dfrac{-3mn-3n+9m+13}{n+1} \end{cases} \tag{8}$$

At the case of m=0, i.e. the Li_2MnO_3 phase does not form, Eqn.(8) is just identical with Eqn.(5). From Eqn.(8), theoretically, the structure properties (such as phase composition, fraction of Li^+ occupied different sites) of $[Li_{1+y}]_{tet}[Mn_{2-x}Li_x]_{oct}O_4$ spinel can be quantitatively analyzed by the data of XRD and the average oxidation state of Mn. The detail for this complex case will be separately discussed in other papers.

It is worth noting that the Li_2MnO_3 phase begins to form even if the value of x does not reach 0.333. For 550 ℃ sample, assuming that the content of Li_2MnO_3 phase is zero (m=0), from its average oxidation state of Mn(3.71), the value of x also is only 0.301. Therefore, during the transfer of Li^+ from tetrahedral 8a sites to octahedral 16d sites, there is a competition between the individual $Li_2Mn_2O_{4+\delta}$ phase ($2x+y=1$) and the multiphase ($2x+y\leqslant 1$) of $[Li_{1+y}]_{tet}[Mn_{2-x}Li_x]_{oct}O_4$ and Li_2MnO_3. Consequently, both of the ideal cubic $Li_2Mn_2O_4$ (x=0, y=1) and ideal lithium-rich $Li_{4+y}Mn_5O_{12}$ phase (y=1) are difficult to be obtained.

In the temperature range of 550-850℃, the TG curve in Fig.5 shows a mass-decreasing process. Note that $[Li_{1+y}]_{tet}[Mn_{2-x}Li_x]_{oct}O_4$ spinel at about 500 ℃ exhibits the stoichiometric $Li_4Mn_5O_{12}$-like structure as discussed above. As suggested by THACKERAY et al[12, 21], the stoichiometric $Li_4Mn_5O_{12}$ would decompose to the more stable $LiMn_2O_4$ and Li_2MnO_3 at temperatures higher than 400 ℃, which is associated with the evacuation of oxygen as follows:

$$Li_4Mn_5O_{12}\rightarrow 2LiMn_2O_4+Li_2MnO_3+1/2O_2 \tag{9}$$

When the sintering temperature is above 900 ℃, the rock-salt $LiMnO_2$ phase can be formed by the reaction between $LiMn_2O_4$ and Li_2MnO_3:

$$LiMn_2O_4+Li_2MnO_3\rightarrow 3LiMnO_2+1/2O_2 \tag{10}$$

From the CV curve of 550 ℃ sample in Fig.4(c), a small redox couple at 3.82 V/3.68 V indicates a little transition from stoichiometric $Li_4Mn_5O_{12}$-like structure to $LiMn_2O_4$-like structure. For the 700 ℃ sample, a large redox couple at 3.86 V/3.66 V in Fig.4(e) suggests that $[Li_{1+y}]_{tet}[Mn_{2-x}Li_x]_{oct}O_4$ spinel with $LiMn_2O_4$-like structure has been largely formed. Because the potential of Li^+ intercalation/ deintercalation in the 4 V region is not observed among the 550−700 ℃ samples, the structure of the these samples is in the middle-phase between $Li_4Mn_5O_{12}$ and $LiMn_2O_4$. In this temperature range, lithium-ions gradually break away from the octahedral 16 d sites to form the Li_2MnO_3 phase, which makes the value of x gradually decrease and the content of Li_2MnO_3 phase further increase. Consequently, the average oxidation state of Mn also decreases with the evacuation of oxygen as shown in Table 2. However, from the CV curve of the 850 ℃ sample in Fig.4(f), only is a weak redox couple at 3.21 V/2.53 V observed, which indicates a phase transition from $LiMn_2O_4$ phase to the rock-salt $LiMnO_2$ phase of which the electrochemical activity is very poor. These results confirm that the reactions as given in Eqn.(9) and Eqn.(10) are also applicable to $[Li_{1+y}]_{tet}[Mn_{2-x}Li_x]_{oct}O_4$ with the non-stoichiometric $Li_4Mn_5O_{12}$-like structure.

4 Conclusions

The composition, structure and electrochemical properties of $Li_2Mn_2O_4$ are very sensitive to the sintering temperature. By the XRD, CV curves and average oxidation state of Mn, the phase transition process of the $Li_2Mn_2O_4$ spinel was investigated. The results show that the transfer of Li^+ from 8a sites to 16d sites plays a very important role in the phase transition of $Li_2Mn_2O_4$. As a result, a series of $[Li_{1+y}]_{tet}[Mn_{2-x}Li_x]_{oct}O_4$ spinels can be formed at different sintering temperatures. In addition, a way of determining x in the $[Li_{1+y}]_{tet}[Mn_{2-x}Li_x]_{oct}O_4$

spinel was also demonstrated by average oxidation state of Mn and the content of Li_2MnO_3.

References

[1] THACHERAY M M. Spinel electrodes for lithium batteries[J]. J Am Ceram Soc, 1999, 82: 3347−3354.

[2] GU Yi-Jie, ZHOU Heng-Hui, CHEN Ji-Tao, CHANG Wen-bao. Effenct of Cr doping on structure of $LiMnO_2$[J]. Trans Nonferrous Met Soc China, 2003, 15: 1217−1219.

[3] LI Yun-Jiao, HONG Shi-Liang, LI Hong-Gui. Structure and electrochemical performance of spinel $LiMn_2O_4$ synthesized by mechanochemical process[J]. Trans Nonferrous Met Soc China, 2005, 15(1): 171−175.

[4] ROBERTSON A D, LU S H, AVERILL W F, Jr HOWARD W F. M^{3+}-modified $LiMn_2O_4$ spinel intercalation cathodes[J]. J Electrochem Soc, 1998, 145: 1131−1136.

[5] TANG Zhi-Yuan, FENG Ji-Jun. Study on spinel $LiMn_{2-x}La_xO_4$ cathode material for lithium-ion batteries[J]. Acta Phys Chim Sin, 2003, 19: 1025−1029. (in Chinese)

[6] PERAMUNAGE D, ABRAHAM K M. Preparation and electrochemical characterization of overlithiated spinel $LiMn_2O_4$[J]. J Electrochem Soc, 1998, 145: 1131−1136.

[7] ENDRES P, FUCHS B, KEMMLER-SACK S, BRANDT K, FAUST-BECKER G, PRAAS H W. Influence of processing on the Li:Mn ratio in spinel phase of the system $Li_{1+x}Mn_{2-x}O_{4-\delta}$ [J]. Solid State Ionics, 1996, 89: 221−231.

[8] OTT A, ENDRES P, KLEIN V, et al. Electrochemical performance and chemical properties of oxidic cathode materials for 4 V rechargeable Li-ion batteries[J]. J Power Sources, 1998, 72: 1−8.

[9] POLOS A I, ANNE A, STROBEL P. Topotactic reactions, structural studies, and lithium intercalation in cation-deficient spinels with formula close to $Li_2Mn_4O_9$[J]. J Solid State Chem, 2001, 160: 108−117.

[10] BLYR A, SIGALA C, AMATUCCI G. Self-discharge of $LiMn_2O_4$/C Li-ion cells in their discharged state[J]. J Electrochem Soc, 1998: 145: 194−209.

[11] GUMMOW R J, LILES D C, THACKERAY M M. Lithium extraction from orthorhombic lithium manganese oxide and the phase transformation to spinel [J]. Mat Res Bull, 1993, 28: 1249−1256.

[12] THACKERAY M M, MANSUETTO M F, JOHNSON C S. Thermal stability of $Li_4Mn_5O_{12}$ electrodes for lithium batteries [J]. J Solid State Chem, 1996, 125: 274−277.

[13] TAKADA T, HAYAKAWA H, AKIBA E. Preparation and crystal structure refinement of $Li_4Mn_5O_{12}$ by the Rietveld method[J]. J Solid State Chem, 1995, 115: 420−426.

[14] ZHANG Y C, WANG H, WANG B, et al. Low temperature synthesis of $Li_4Mn_5O_{12}$ nanocrystalline by a hydrothermal method[J]. Mater Res Bull, 2002, 37: 1411−1417.

[15] TANG Xin-Cun, HE Li-Ping, CHEN Zong-Zhang, JIA Dian-zeng, XIA Xi. Structure, preparation mechanism and thermo-decomposition process of $LiMn_2O_4$ precursor prepared by low-heating solid-state reaction[J]. Chem J Chinese Universities, 2003, 24: 576−579. (in Chinese)

[16] TANG Xin-Cun, YANG You-Ping, LI Li-Qing, JIA Dian-zeng, HUANG Ke-long. Preparation of spinel $LiMn_2O_4$ by thermo-decomposition of $LiMn_2L(Ac)_2$ and its electrochemical properties[J]. The Chinese Journal of Nonferrous Metals, 2004, 14(5): 871−876. (in Chinese)

[17] JULIEN C M, MASSOT M. Lattice vibrations of materials for lithium rechargeable batteries III. Lithium manganese oxides[J]. Mater Sci Eng B, 2003, 100: 69−78.

[18] KALYANI P, CHITRA S, MOHAN T, GOPUKUMAR S. Lithium metal rechargeable cells using Li_2MnO_3 as the positive electrode[J]. J Power Sources, 1999, 80: 103−106.

[19] LEE Y S, YOSHIO M. Preparation of orthorhombic $LiMnO_2$ material by quenching[J]. Electrochem Solid-state Lett 2001, 4(10): A166−A169.

[20] TAKADA T, ENOKI H, HAYAKAWA H, AKIBA E. Novel synthesis process and structural characterization of Li-Mn-O spinels[J]. J Solid State Chem, 1998, 139: 290−298.

[21] THACKERAY M M, MANSUETTO M F, DEES D W, VISSERS D R. The thermal stability of lithium-manganese-oxide spinel phases[J]. Mater Res Bull, 1996, 31: 133−140.

(Edited by LI Xiang-qun)